Philippine Engineering Journal (2002) XXII1 (2): 35-48

SYNTHESIS OF PB-FREE BI-2223 FROM BI-2212 USING PARTIAL MELTING

M.U. Herrera and R.V. Sarmago
Material Science and Engineering Program, College of Science
University of the Philippines, Diliman, Quezon City
Tel No.: 4344260; Fax No. 9205474
Email: muherrera@yahoo.com

ABSTRACT

Synthesis of Pb-free Bi-2223 has been made possible by partial melting. Partial melting was done by sintering the samples below the melting point of Bi-2212 thus allowing the dissociation of the weak bonds of BiO layer to exhibit fluid-like planar movements. Volume fraction of Bi-2223 increases with temperature which was attributed to the increase in fluid-like movements. Also, the samples sintered at long sintering time of 50hrs and 100hrs show larger volume fraction of Bi-2223 as compared with those sintered at 25hrs. The involvement of fluid-like planar movements during the partial melting process was supported by the presence of fused-grain boundaries, layered structure, and hole-like features seen in the Scanning Electron Microscopy images.

I. Introduction

$Bi_2Sr_2Ca_2Cu_3O_x$ (Bi-2223) has a critical temperature of 110K. Its high critical temperature makes it a promising material for superconducting cables and wires that can be operational above the boiling point of nitrogen. Along with its potential is the difficulty of its synthesis due to its complex structure. The difficulty of its synthesis can be minimized by the addition of lead. Thus, most of the physical properties in literature are taken from Pb-doped samples and lead free samples are still a rarity. Furthermore, there is still a need to know the effect of lead on the physical and superconducting properties of Bi-2223 and this could be made possible if ample amounts of Pb-doped and Pb-free samples are available.

Pb-free Bi-2223 is difficult to synthesize. It has a sluggish formation process (Zhu, et. al, 1999, Huang, 1998) and narrow phase stability. Researchers such as Yu (1996) claimed to be able to synthesize Pb-free Bi-2223 but the samples were prepared for 16 days. The very long sintering time of the procedure is very difficult to achieve. Thus, there is a need to explore for better method of synthesizing Pb-free Bi-2223.

The main objective of this paper is to synthesize Pb-free Bi-2223 from $Bi_2Sr_2CaCu_2O_x$ (Bi-2212) precursor using partial melting The use of Bi-2212 as a precursor is based on intercalation model (Garnier, 2000, Zhu, 1999) in which Bi-2212 is converted directly to Bi-2223 by the insertion of Ca-Cu-O units. This avoids series of

transformational changes from oxides/carbonates precursor to Bi-2223 that include the formations of Bi-2201 and Bi-2212 as intermediate phases before becoming Bi-2223. On other hand, the method of partial melting is based on reports that improvement in the amount of Bi-2223 is associated with the presence of a partially melted phase (liquid phase, molten phase, or fluid-like movement) (Khaled, et. al 1996, Hadano et. al., 1988; Oka et. al., 1989, Shimojima et. al., 1989, Ono, 1988, Uzumaki, 1989, Aota, 1989).

In this study, partial melting of Bi-2212 was done below the melting point of Bi-2212. This method utilizes the two-dimensional anisotropy of Bi-2212 in which it is expected that the a,b planes having a lower bonding energy melt at a lower temperature than the c - directions. In this particular case, the BiO layer bonds of Bi-2212 are weaker (Majewski, 2000, Matsui, 1988) than in the other directions, thus they dissociate before the actual melting point of Bi-2212. When these bonds dissociate, Bi-2212 could move more freely along the a,b plane, thus, there is high probability to react with other precursors (Ca_2CuO_3 and CuO) to form Bi-2223. By partial melting, the slow solid-state reaction is improved by the introduction of fluid-like movements for faster precursor movements.

II. Methodology

2.1. Preparation of Bi-2212 and Ca_2CuO_3

Bi-2212 and Ca_2CuO_3 were prepared via solid state sintering. The chemical reactions involved in the synthesis are as follows:

$$Bi_2O_3 + 2SrCO_3 + CaCO_3 + 2CuO \rightarrow Bi_2Sr_2CaCu_2O_8 + 3CO_2$$

$$2CaCO_3 + CuO \rightarrow Ca_2CuO_3 + 2CO_2$$

Stoichiometric amounts of oxide and carbonate precursors were mixed and ground in an agate until the mix became homogenous. The reagents used as precursors of Bi-2212 and Ca_2CuO_3 are presented in Table 1. The mixtures were placed in a mold and pressed into pellet from using a hydraulic press with a pressure of 10MPa. Each pellet was placed in an alumina boat and sintered in a furnace for 100-hrs. Bi-2212 was sintered at 830°C while Ca_2CuO_3 was sintered at 900°C.

Table 1.
Reagents used as precursors of Bi-2212 and Ca_2CuO_3

Reagent	Brand Name	Percent Purity
Bi_2O_3	Fluka	>98%
$SrCO_3$	Baker Analyzed	99.4%
$CaCO_3$	Fluka	99%
CuO	Alfa Aesear	99.7%

2.2. *Synthesis of Bi-2223*

Stoichiometric amounts of Bi-2212, Ca_2CuO_3 and CuO were mixed and ground in an agate until they became homogenous. Partial melting was achieved by sintering the sample at temperatures below the melting point of Bi-2212. The temperature range of 865°C - 870°C was chosen as sintering temperature since this is close to the peak of the endothermic curve (Lui, 1998) that correspond to melting of Bi-2212 at 874.1°C. The samples were also sintered at different sintering times ranging from 25hrs to 100hrs.

2.3. *Electric Characterization of the Sample*

A four-point probe apparatus was used to determine the sample resistance in a closed-cycle helium cryostat. In the four-point probe set-up, the two terminals at the opposite ends were intended for the passage of current while the two inner wires were for voltage measurements. The samples were cut into bars, and then four gold wires were soldered using indium contact. The voltage drop across the two intermediate wires was proportional to the resistance of the sample.

The graph of resistance vs. temperature shows the critical temperature of the samples that would verify the existence of the superconducting phase. When the sample is in the normal state, it has a non-zero resistance. The trend in the graph abruptly changes at the critical temperature, Tc, dropping to zero at its superconducting state. The critical temperatures of the sintered samples were estimated as the point of intersection of two extrapolated lines from the normal state and from the resistance drop. The two-step drops in the resistance vs. temperature show the presence of two superconducting phases in the sample. The drop in total resistance at the higher temperature is due to the abrupt change in resistance when the high-Tc phase becomes superconducting. The drop at lower temperature is due to the abrupt change in resistance when the low-Tc phase becomes superconducting. The ratio of the drop due to high-Tc and low-Tc phase is affected by the relative proportion of the two phases in the conducting path.

2.4. *Magnetic Characterization of the Sample*

A Hartshorn configuration mutual inductance bridge was used to measure the ac magnetic susceptibility in a closed-cycle helium cryostat. The Mutual Inductance Bridge consists of a primary coil and two secondary coils. A function generator supplies the AC signals to the primary coils that produce the AC magnetic field, while a lock-in amplifier detects the output signal of the two secondary coils. The magnetic susceptibility of the sample was proportional to the voltage across the secondary coils.

The graph of ac magnetic susceptibility vs. temperature shows the critical temperature of the sintered samples that would verify the existence of the superconducting phase. When the sample is in the normal state, the sample is

paramagnetic. The trend in the graph abruptly changes at the critical temperature, Tc, until the susceptibility becomes –1 showing a state of perfect diamagnetism.

2.5. X-ray Diffraction

X-ray diffraction was used to detect the existence of Bi-2223 in the samples. Samples were ground in an agate mortar to ensure random orientation of the grains. It was then mounted in a sample holder and pressed lightly to obtain a powder compact. Background radiation was subtracted from the data and diffraction peak intensities were normalized so that the highest intensity has a value of one.

2.6. Scanning Electron Microscopy

The fractured samples were mounted on a sample holder using a carbon tape. It was then placed under a scanning electron microscope for the investigation of its topological features.

III. Results and Discussion

Figure 1 shows the graph of resistance vs. temperature of the sample sintered for 50-hrs at different temperatures. The sample sintered at 865°C (figure 1A) has two transition temperatures. The transition at 110K indicates the presence of Bi-2223 and the transition at 69K indicates the presence of Bi-2212. The sample sintered at 868°C (figure 1B) also has two transition temperatures. The transitions at 75K and 109K show the presence of Bi-2212 and Bi-2223, respectively. The sample sintered at 870°C (figure 1C) has a transition temperature at 111K. This transition temperature corresponds to the presence of Bi-2223 in the sample. It is obvious from the graph in figure 1, that the drop in resistance due to the high-Tc phase (Bi-2223) is largest for the sample sintered at 870°C. This suggests that this sample possesses the largest amount of Bi-2223.

Figure 2 shows the graph of resistance vs. temperature of the samples sintered at 870°C for different times. The sample sintered for 25-hrs (figure 2A) has two transition temperatures that are at 74K and 108K. These critical temperatures correspond to Bi-2212 and Bi-2223, respectively. The samples sintered for 50-hrs (figure 2B) and 100-hrs (figure 2C) have transition temperatures at 108K and 110K, respectively. This confirms the existence of Bi-2223 in the samples. The graph in figure 2 shows that the samples sintered at longer sintering time for 50-hrs and 100-hrs possesses electrical characteristics related to Bi-2223.

Figure 3 shows the graph of in-phase susceptibility, χ vs. temperature of the sample sintered for 50-hrs at different temperature. The sample sintered for 865°C (figure 3A) has a critical temperature of 68K. This is consistent with the data from the resistance vs. temperature that the sample sintered at 865°C is mainly composed of Bi-2212. The samples sintered at 868°C (figure 3B) and 870°C (figure 3C) have critical temperatures of 97K and 101K, respectively. These are consistent with the data from the resistance vs. temperature that Bi-2223 is present in the samples.

Figure 4 shows the graph of in-phase susceptibility, χ vs. temperature of the sample sintered at 870°C for different times. The sample sintered for 25-hrs (figure 4A) has transition temperature of 76K. This is consistent with the data from the resistance vs. temperature that the sample sintered for 25-hrs is composed mainly of Bi-2212. The samples sintered for 50-hrs (figure 4B) and 100-hrs (figure 4C) have transition temperatures 101K and 113K, respectively. These are consistent with the data from the resistance vs. temperature that Bi-2223 is present in the samples.

The X-ray diffraction measurements further verified the existence of Bi-2223 in the samples showing the success of partial melting in the synthesis Pb-free Bi-2223. Figure 5 shows the intensity of (115) planes of Bi-2223 samples, which is proportional to the volume fraction of Bi-2223 in the sample. The large volume fractions of Pb-free Bi-2223 can be seen at samples sintered at 870°C for 50-100hrs.

Bi-2223 volume fraction increases with sintering temperature and was largest at 870°C, this agrees with the results of electrical and magnetic measurements. The sintering temperature of 870 °C is part of the curve of the endothermic peak of Bi-2212 that corresponds to melting as shown in the DTA curve of Bi-2212 as presented in the works by Lui (1998). The increase in volume fraction as sintering temperature approaches the melting point of Bi-2212 could be explained by the increase in fluid-like movements with temperature until the material behaves totally like a fluid at its melting point. Comparing with the results of Pb-doped samples presented in the works of Herrera (2002), a similar trending were observed in that Pb-doped Bi-2223 volume fraction were largest near the melting point of Pb-doped Bi-2212.

Figure 6 shows the SEM images of the sample sintered at 865°C, 868° C, and 700°C. As observed from the SEM image of samples sintered at 865°C (figure 6A) there are unfused grain boundaries and the grains were stacked with each other. On other hand, the samples sintered at 868°C (figure 6B) and 700°C (figure 6C) shows fused grain boundaries. Figure 7 shows fused grain boundaries that signify that the grains have become very soft and have attained liquid-like properties. Figure 8 shows the presence of layered structure or terrace-like structure on the samples sintered above 868°C. The layered structures indicate planar movements as shown by the displacement of one layer with respect to other layers. The sliding of layers supports the existence of fluid-like planar movements during the synthesis process. The layered structures also show ordered crystalline structure within a layer showing that bonding along a,c plane and b,c plane are still not dissociated.

Figure 9 shows the presence of hole-like features (pores) on the samples sintered above 868°C. The presence of hole-like features support the existence of planar movement in the sample. Figure 10 illustrates formation of hole-like features as viewed in a,b plane. Figure 10a shows Bi-2212 grains undergoing fluid-like planar movement when it is nearly touching other grains that undergoes the same process. Figure 10b shows that the grain boundaries of the lower layers are touching other grain boundaries while the upper layers nearly touch other grain boundaries. Figure 10c shows that the moving grains completely touch other grain boundaries forming fused grain boundaries.

The presence of fused grain boundaries, terrace-like features and hole-like structure were also used to support the existence of partial melting in the Pb-doped Bi-2223 (Herrera, 2002).

IV. Summary and Conclusion

Synthesis of Pb-free Bi-2223 has been made possible by partial melting. This was done by sintering the samples below the melting point of Bi-2212 allowing the dissociation of the weak bonds of BiO bilayers. The dissociation of the BiO layers bonds favors the fluid-like planar movements along the a-b plane which facilitates faster reaction. Samples that are sintered at temperatures where partial melting of grains occur show improvement of Bi-2223 volume fraction as compared to those samples that are not. Also, samples sintered at higher temperature show larger Bi-2223 volume fraction that is attributed to the increase in the fluid-like movement. Electrical and magnetic characteristics were obtained to confirm the superconducting properties of the samples.

V. References

1. K. Aota, H. Hattori, T. Hatano, K. Nakamura, K. Ogawa, Growth of the 2223 Phase in Leaded Bi-Sr-Ca-Cu Oxide under Reduced Oxygen Partial Pressure, *Japanese Journal of Applied Physics*, 28(12), L2196-L2199 (1989).
2. Garnier, I. Monet-Laffez, G. Desgardin, Kinetics study of the Bi-2223 grain growth thickness, *Physica C*, 349, (2000).
3. T. Hadano, K. Aota , S. Ikeda, K. Nakamura, K. Ogawa, Growth of the 2223 Phase in Leaded Bi-Sr-Ca-Cu-O System, *Japanese Journal of Applied Physics*, L2055-L2058 (1988).
4. M. Herrera, R.V. Sarmago, Synthesis of Pb-doped Bi-2223 from Pb-doped Bi-2212, Ca_2CuO_3 and CuO above the Glass Transition Temperature of Bi-2212**,** *Science Diliman: A Journal of Pure and Applied Sciences***, 14, 2, (2002).**
5. Y. Huang, D.S. Shy, L.J. Chen, Phase evolution of co-precipitated Bi-Pb-Sr-Ca-Cu-O powder, *Physica C*, 294, 140-146 (1998).
6. J. Khaled, T. Komatsu, K. Matusita, A new model for the formation of high-Tc phase in superconductive $(Bi,Pb)_2Sr_2Ca_2Cu_3O_x$ glass-ceramics, *Journal of Material Science: Materials Electronic*, 7, 261-266 (1996).
7. H. Liu, L.Liu, Y. Zhang, Z. Jin, Effects of Pb and Ca on the melting point of the 2212 phase in the (Bi,Pb)SrCaCuO system, *Journal of Material Science Letter*, 17, 665-667 (1998).
8. P. Majewski, P, 2000, Material aspects of the high-temperature superconductors in system Bi_2O_3-SrO-CaO-CuO, *Journal of Material Research,* 15(4), 854-870 (2000).
9. Y. Matsui, S. Horiuchi, Geometrical Relations of Various Modulated Structures in Bi-Sr-Ca-Cu-O Superconductors and Related Compounds, *Japanese Journal of Applied Physics,* 27(12), L2306-L2309 (1988).
10. Y. Oka, N. Yamamoto, H. Kitaguchi, K. Oda, J. Takada, 1989. Crystallization Behavior and Partially Melted States in Bi-Sr-Ca-Cu-O, *Japanese Journal of Applied Physics,* 28(2), L213-L216 (1989).
11. Ono, Crystallization of 107K Superconducting Phase and Partial Melting in the Bi-(Pb)-Sr-Ca-Cu-O System. Japanese Journal Applied Physics, 27(12), L2276-L2279 (1988).
12. H. Shimojima, K. Tsukamoto, C. Yamagishi, Preparation of the High-Tc Superconductive Bi-Pb-Sr-Ca-Cu-O Film Pylolysis of Organic Acid Salts, *Japanese Journal of Applied Physics,* 28(2), L226-L228 (1989).

13. T. Uzumaki, K. Yamanaka, N. Kamehara, K. Niwa, The effect of Ca2PbO4 Addition on superconductivity in a Bi-Sr-Cu-O System, *Japanese Journal of Applied Physics,* 26(1), L75-L77 (1989).
14. S. Yu, Y. Okuda, E. Takayama-Muromachi, Critical Current Densities and Irreversibility Fields in Pb-doped and Pb-free $Bi_2Sr_2Ca_2Cu_3O_y$ Superconductors, *Japanese Journal of Applied Physics,* 35, 2619-2623 (1996).
15. W. Zhu, C. Kuo, P. Nicholson, Diffusion calculations for the 80-Kto-110K Bi(Pb)SrCaCuO Superconducting phase formation, *Journal of Material Research*, 14(11), 4143-4147 (1999).

Nomenclature

Symbol	Description	Units
Bi-2223	$Bi_2Sr_2Ca_2Cu_3O_x$	
Bi-2212	$Bi_2Sr_2CaCu_2O_x$	
χ	Magnetic Susceptibility	unitless
Tc	Critical Temperature	Kelvin

Figures

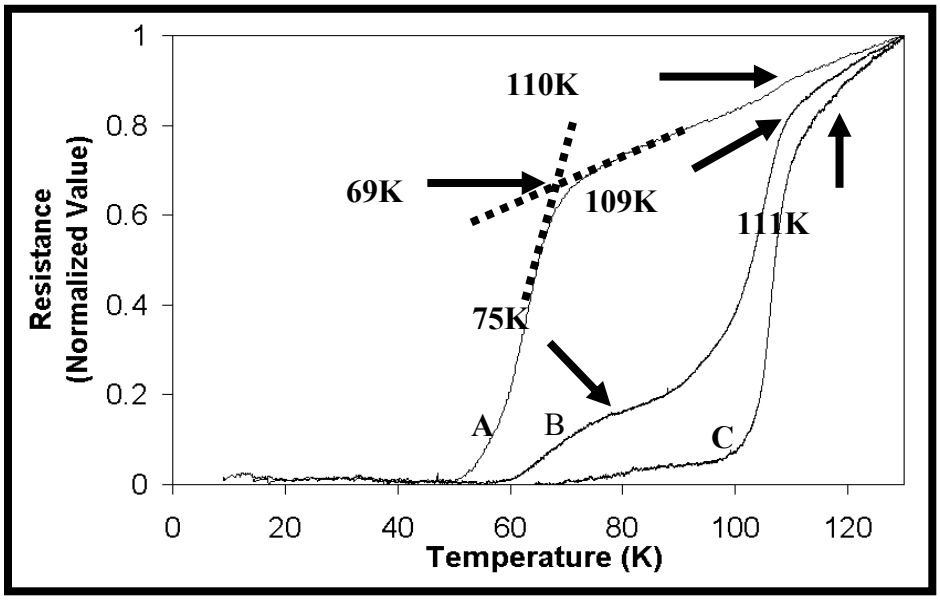

Figure 1. Resistance vs. Temperature of the samples sintered for 50hrs at A) 865ºC, B) 868ºC and C) 870ºC

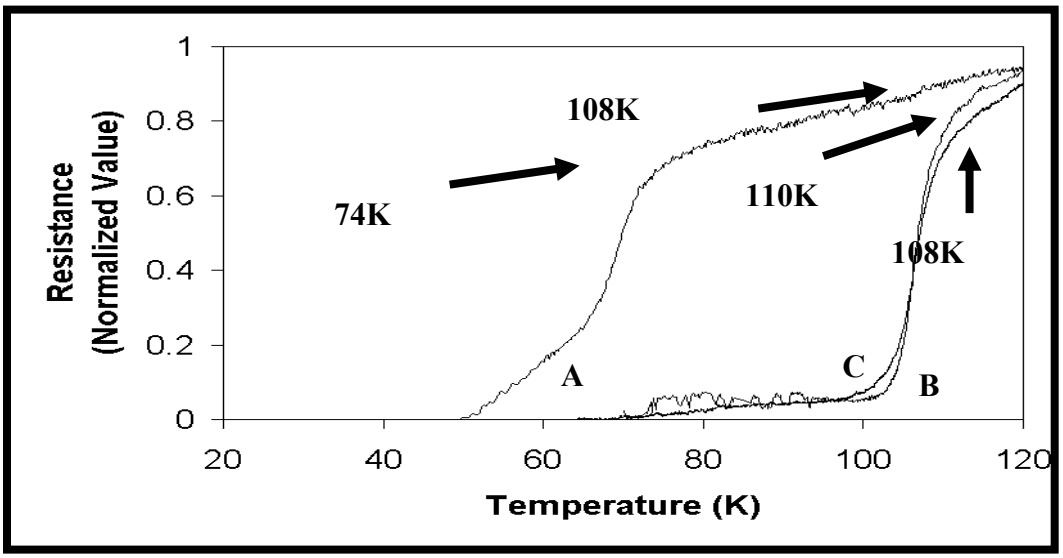

Figure 2. Resistance vs. Temperature of the samples sintered at at 870°C for A) 25-hrs, B) 50-hrs and C) 100hrs

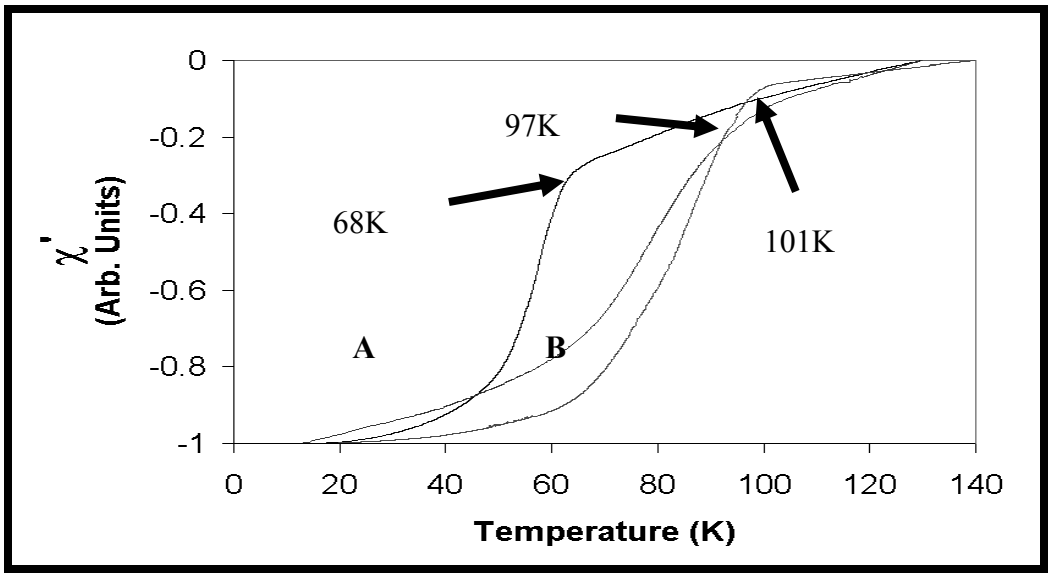

Figure 3. In-phase Susceptibility vs. Temperature of the samples sintered for 50hrs at A) 865°C, B) 868 °C and C) 870°C

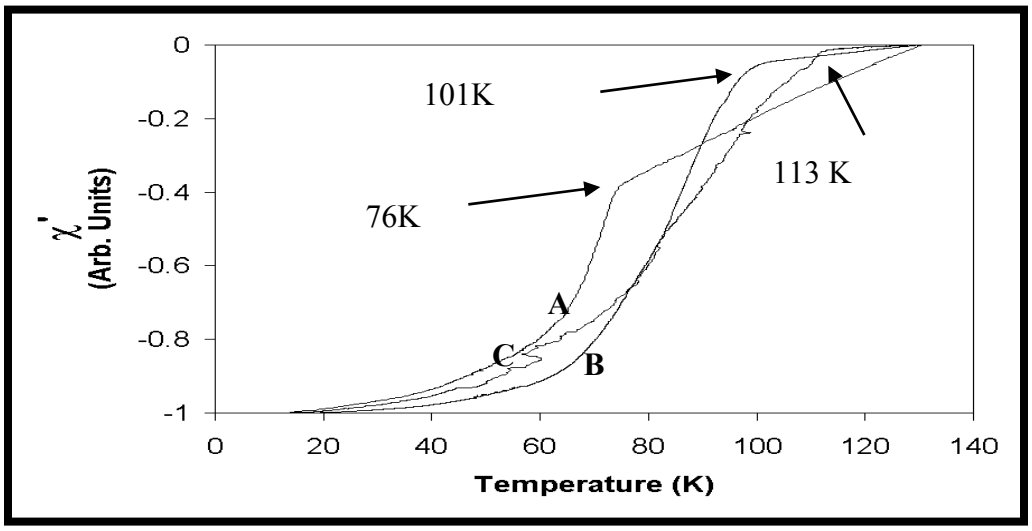

Figure 4. In-phase Susceptibility vs. Temperature of the samples sintered at 870°C for A) 25-hrs, B) 50-hrs and C) 100hrs.

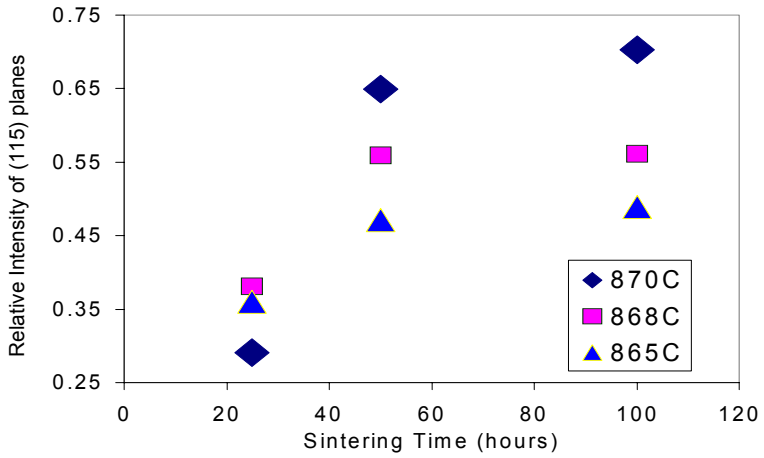

Figure 5. Intensity of (115) plane for sample sintered at a particular sintering temperature and time

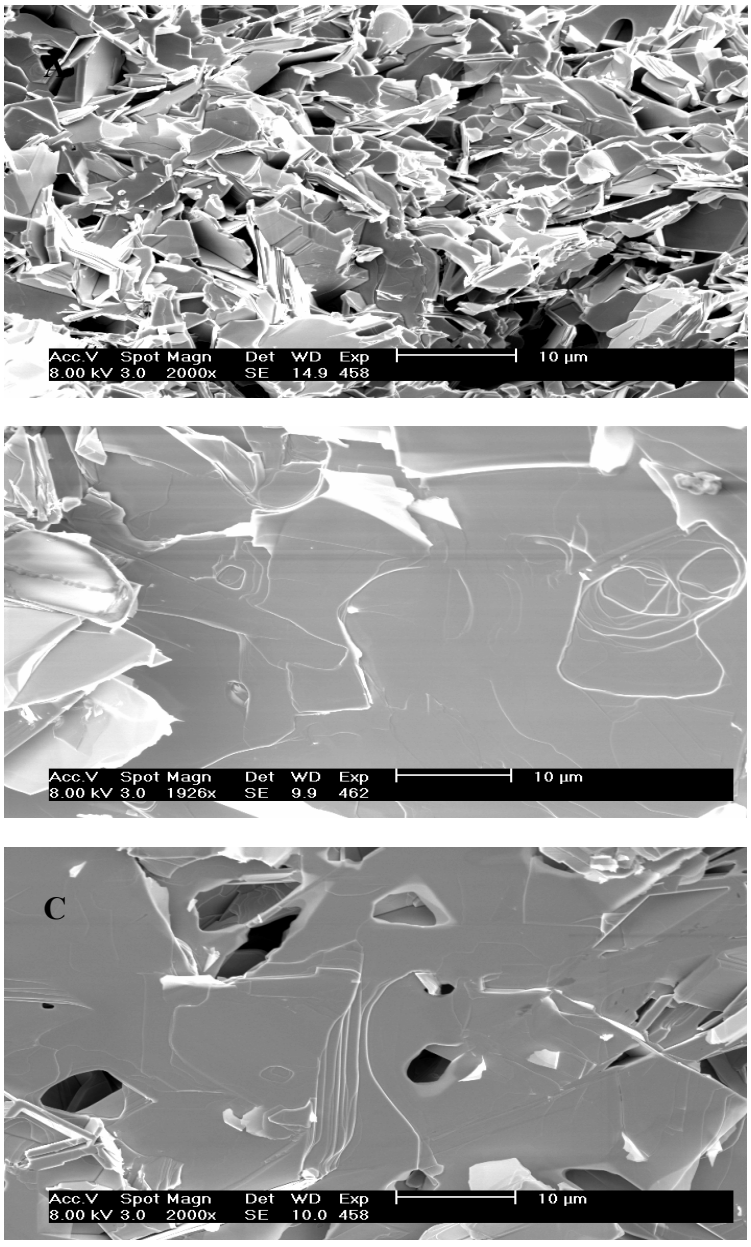

Figure 6. SEM image of sample sintered at 865°C, 868°C, and 870°C

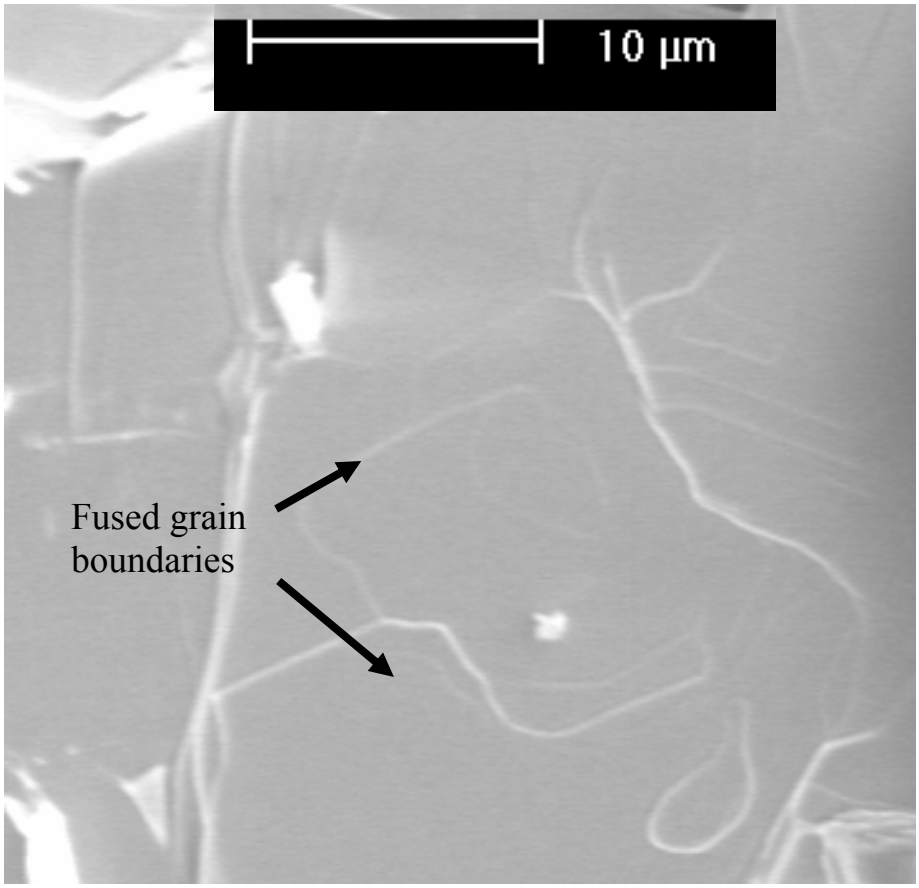

Figure 7. Fused grains boundaries

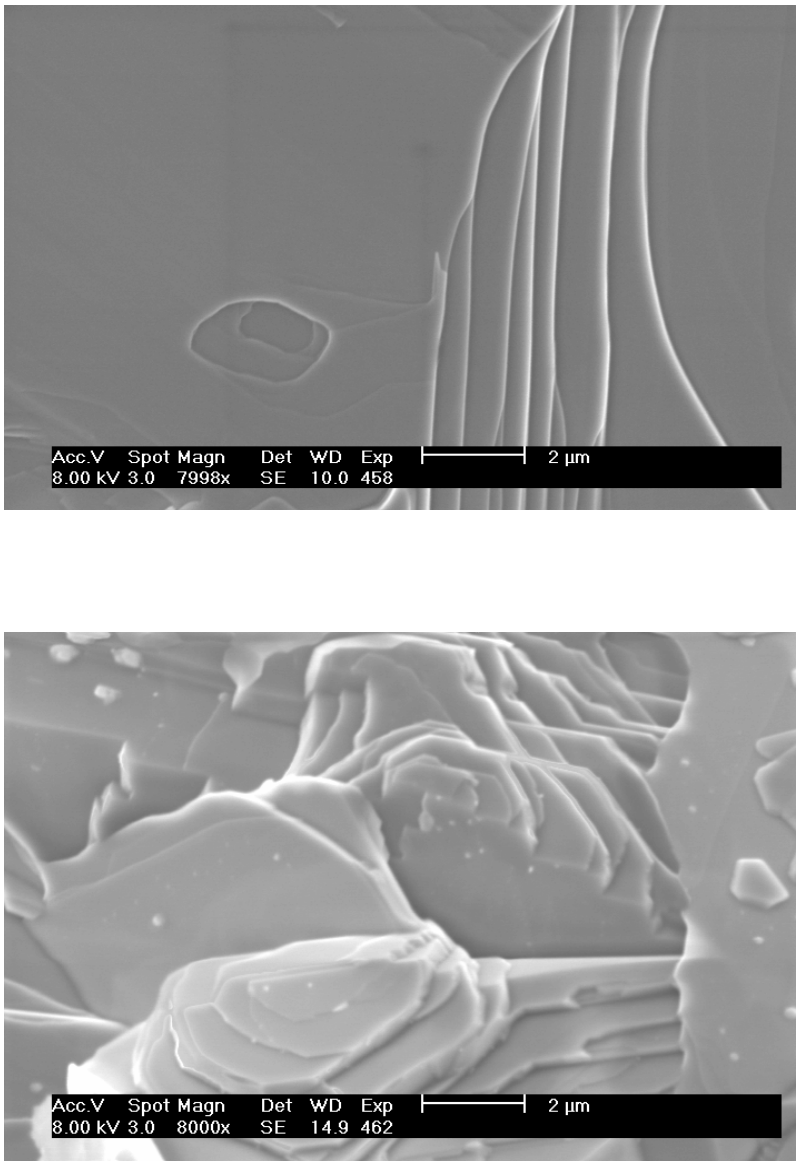

Figure 8. Layered Structure

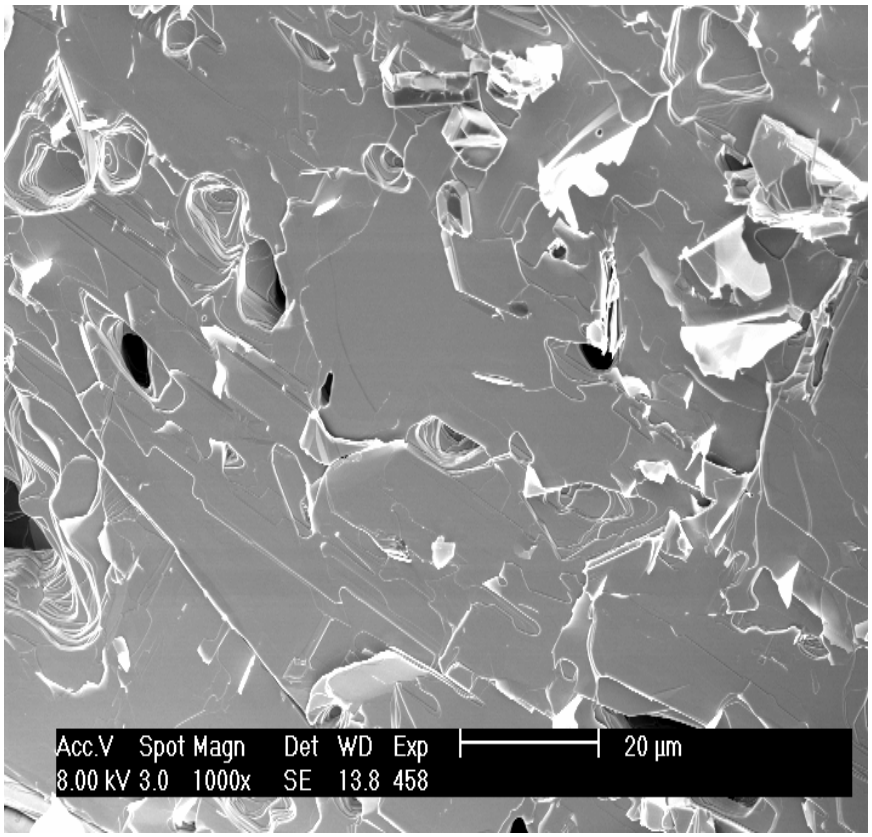

Figure 9. Hole-like structure

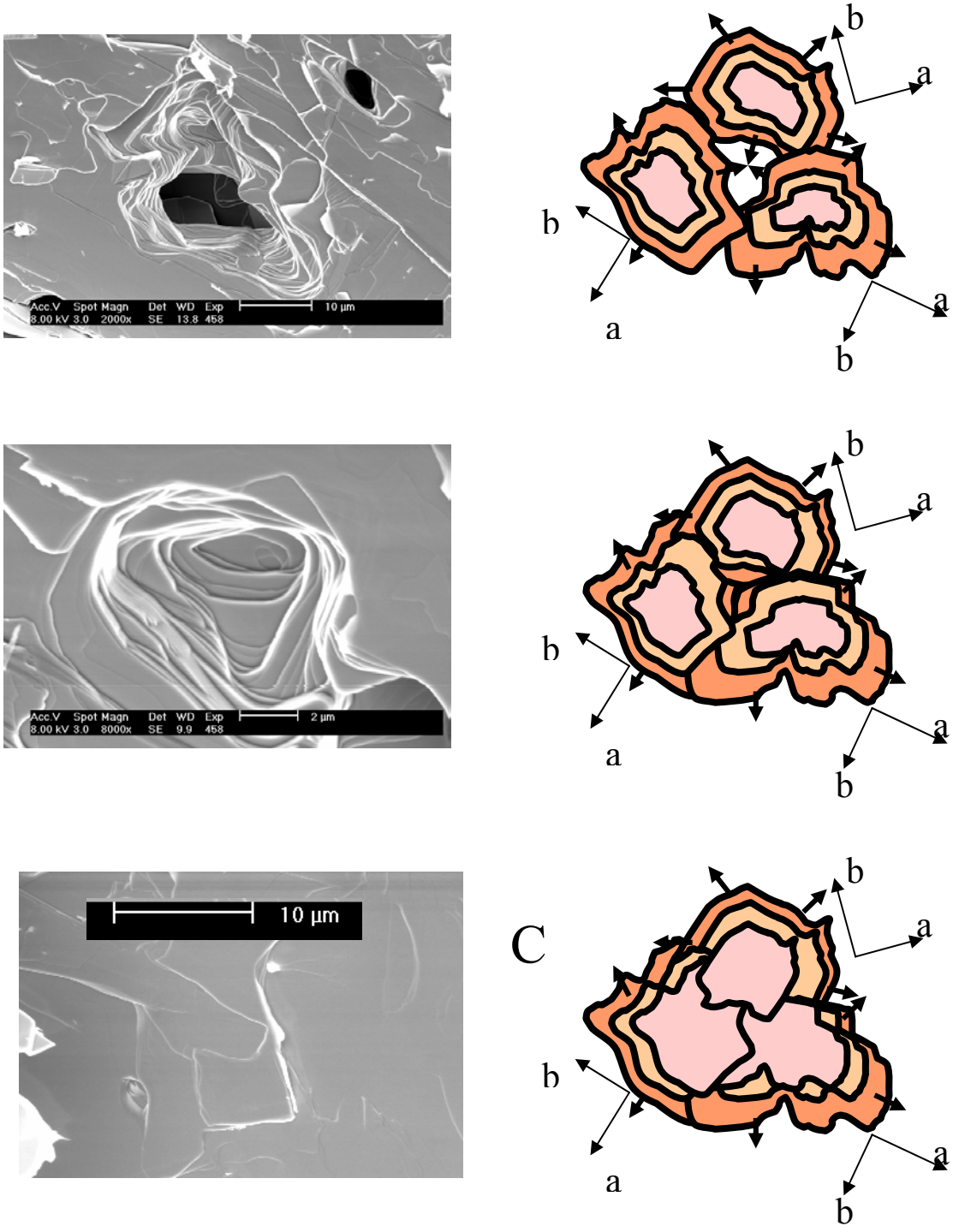

Figure 10. Bi-2212 grains undergoing fluid-like planar movement nearly touching other grains that undergo the same process, B) The grain boundaries of the lower layers touch other grain boundary while the upper layers nearly touch other grain boundary, C) moving grains completely touch other grain boundaries forming fused grain boundaries.